第 32 卷第 5 期
2016 年 5 月

无 机 化 学 学 报
CHINESE JOURNAL OF INORGANIC CHEMISTRY

Vol.32 No.5
853-858

配位聚合物$[Fe(HL)(H_2O)]_n$的合成、晶体结构及磁性质

赵素琴*,[1] 顾金忠*,[2]

([1]青海民族大学物理与电子信息工程学院,西宁 810007)

([2]兰州大学化学化工学院,兰州 730000)

摘要:通过水热方法,采用 H_3L(H_3L=2-(4-carboxypyridin-3-yl)terephthalic acid)与 $FeSO_4·7H_2O$ 反应,合成了一个具有二维结构的配位聚合物$[Fe(HL)(H_2O)]_n$ (**1**),并对其结构和磁性质进行了研究。结构分析结果表明该聚合物的晶体属于正交晶系,*Pnna* 空间群,a=1.454 65(11) nm,b=2.474 23(15) nm,c=0.735 65(4) nm,V=2.647 7(3) nm^3,D_c=1.802 g·cm^{-3},Z=8,R=0.046 8,wR=0.125 6($I>2\sigma(I)$)。HL^{2-}配体交替连接相邻的铁(Ⅱ)离子形成了一维链结构单元,这些链又通过配体与铁(Ⅱ)离子的配位作用形成了二维层。最后这些层通过氢键作用形成了一个复杂的三维超分子框架。拓扑分析表明,配合物 **1** 具有一个双节 4,4-连接的拓扑网络结构,其拓扑符号为($4^3.6^2.8$)。研究表明,该聚合物中相邻铁(Ⅱ)离子之间存在反铁磁相互作用。

关键词:配位聚合物;铁(Ⅱ)配合物;磁性

中图分类号:O614.81+1 **文献标识码**:A **文章编号**:1001-4861(2016)05-0853-06

DOI:10.11862/CJIC.2016.114

Synthesis, Crystal Structure and Magnetic Property of a Coordination Polymer $[Fe(HL)(H_2O)]_n$

ZHAO Su-Qin*,[1] GU Jin-Zhong*,[2]

([1]*College of Physics and Electronic Information Engineering, Qinghai University for Nationalities, Xining, Qinghai* 810007, *China*)

([2]*College of Chemistry and Chemical Engineering, Lanzhou University, Lanzhou* 730000, *China*)

Abstract: A coordination polymer, namely $[Fe(HL)(H_2O)]_n$ (**1**), has been synthesized hydrothermally using H_3L (H_3L=2-(4-carboxypyridin-3-yl)terephthalic acid) and $FeSO_4·7H_2O$. The compound crystallizes in the orthorhombic system, space group *Pnna* with a=1.454 65(11) nm, b=2.474 23(15) nm, c=0.735 65(4) nm, V=2.647 7(3) nm^3, D_c=1.802 g·cm^{-3}, Z=8, R=0.046 8 and wR=0.125 6 ($I>2\sigma(I)$). The HL^{2-} moieties alternately link the adjacent Fe(Ⅱ) centers to form a 1D chain motif. These 1D motifs are arranged into a 2D sheet structure by further coordination interactions of the HL^{2-} ligands to Fe(Ⅱ) ions. Furthermore, the neighboring metal-organic sheets in **1** are assembled, through the O–H···O hydrogen bonds, into a complex 3D supramolecular framework. For topological analysis, the 2D metal-organic network in **1** is a binodal 4,4-connected layer, which is defined by the point symbol of ($4^3.6^2.8$). Magnetic studies for compound 1 show a weak antiferromagnetic coupling between the nearest Fe(Ⅱ) centers, with g=2.04 and J=−2.57 cm^{-1}. CCDC: 1437796.

Keywords: coordination polymer; iron(Ⅱ) complex; magnetic properties

收稿日期:2015-11-21。收修改稿日期:2016-04-02。

青海省应用基础研究计划项目(No.2015-ZJ-738)资助。

*通信联系人。E-mail:qhzhsq@sina.com,gujzh@lzu.edu.cn;会员登记号:S06N5892M1004。

0 Introduction

Recently, the design and synthesis of transition metal functional coordination polymers have received enormous attention for their appealing structural topologies as well as potential applications such as gas storage, magnetism, luminescence and catalysis, etc[1-6]. However, it is still a great challenge to generate compounds with desirable structural features and properties, since a lot of factors can influence the result, such as coordination geometries of metal ions, main organic ligands, introduction of auxiliary ligands, variation in reaction temperatures, ratios of reagents, types of solvents, pH values, crystallization conditions, etc[7-12]. In this regard, diverse multicarboxylic or heterocyclic carboxylic acids are frequently used as multifunctional building blocks in generating coordination polymers, not only because of their ability to lead to different coordination modes and exhibit high thermal stability, but also due to their possibility to act as good H-bond donors and acceptors[3-5,13-16]. In order to extend our investigations in this field, we chose 2-(4-carboxypyridin-3-yl)terephthalic acid (H_3L) as a functional ligand, based on the following considerations: first, H_3L should be an excellent bridging ligand for the construction of coordination polymers, since it has diversified coordination modes and flexible conformation, in which pyridyl and phenyl rings can rotate around the C-C bond; second, to the best of our knowledge, H_3L ligand has not been adequately explored in the construction of coordination polymers. Herein, we report the synthesis, crystal structure, magnetic properties of Fe(Ⅱ) compound with H_3L ligand.

1 Experimental

1.1 Reagents and physical measurements

All chemicals and solvents were of AR grade and used without further purification. Carbon, hydrogen and nitrogen were determined using an Elementar Vario EL elemental analyzer. IR spectra were recorded using KBr pellets and a Bruker EQUINOX 55 spectrometer. Thermogravimetric analysis (TGA) data were collected on a LINSEIS STA PT1600 thermal analyzer with a heating rate of 10 ℃·min^{-1}. Powder X-ray diffraction patterns (PXRD) were determined with a Rigaku-Dmax 2400 diffractometer using Cu $K\alpha$ radiation (λ =0.154 060 nm) and 2θ ranging from 5° to 45°, in which the X-ray tube was operated at 40 kV and 40 mA. Magnetic susceptibility data were collected in the 2~300 K temperature range with a Quantum Design SQUID Magnetometer MPMS XL-7 with a field of 0.1 T. A correction was made for the diamagnetic contribution prior to data analysis.

1.2 Synthesis of the title complex

A mixture of $FeSO_4·7H_2O$ (0.083 g, 0.3 mmol), H_3L (0.073 g, 0.3 mmol), NaOH (0.024 g, 0.6 mmol), and H_2O (10 mL) was stirred at room temperature for 15 min, and then sealed in a 25 mL Teflon-lined stainless steel vessel, and heated at 160 ℃ for 3 days, followed by cooling to room temperature at a rate of 10 ℃·h^{-1}. Red block-shaped crystals of **1** were isolated manually, and washed with distilled water. Yield: 60% (based on Fe). Anal. Calcd. for $C_{14}H_9FeNO_7$ (%): C 46.83, H 2.53, N 3.90; Found(%): C 46.52, H 2.51, N 3.95. IR (KBr, cm^{-1}): 3 601m, 3 422m, 1 716s, 1 588s, 1 548s, 1 480w, 1 388vs, 1 290w, 1 238m, 1 170w, 1 124 w, 1 038w, 946w, 860w, 814w, 784w, 744m, 698m, 664 w, 566w, 486w.

The compound is insoluble in water and common organic solvents, such as methanol, ethanol, acetone, and DMF.

1.3 Structure determination

Single-crystal data of compound **1** were collected at 293 (2) K on a Bruker Smart Apex 1000 CCD diffractometer with Cu $K\alpha$ radiation (λ=0.154 184 nm). A summary of the crystallography data and structure refinement is given in Table 1, and selected bond lengths and angles are listed in Table 2. The structures were solved using direct methods, which yielded the positions of all non-hydrogen atoms. These were refined first isotropically and then anisotropically. All the hydrogen atoms were placed in calculated positions with fixed isotropic thermal parameters and included in structure factor calculations in the final stage of full-matrix least-squares refinement. All

Table 1　Crystal data for compound 1

Compound	**1**	Crystal size / mm	0.26×0.25×0.20
Chemical formula	$C_{14}H_9FeNO_7$	θ range for data collection / (°)	6.08~70.95
Molecular weight	359.07	Limiting indices	$-17 \leqslant h \leqslant 17$, $-30 \leqslant k \leqslant 27$, $-8 \leqslant l \leqslant 7$
Crystal system	Orthorhombic	Reflections collected, unique (R_{int})	12 823, 2 478 (0.068 6)
Space group	*Pnna*	D_c / (g·cm^{-3})	1.802
a / nm	1.454 65(11)	μ / mm^{-1}	9.537
b / nm	2.474 23(15)	Data, restraints, parameters	2 478, 0, 210
c / nm	0.735 65(4)	Goodness-of-fit on F^2	1.054
V / nm^3	2.647 7(3)	Final R indices ($I \geqslant 2\sigma(I)$) R_1, wR_2	0.046 8, 0.125 6
Z	8	R indices (all data) R_1, wR_2	0.060 8, 0.141 4
F(000)	1 456	Largest diff. peak and hole / (e·nm^{-3})	448 and −671

Table 2　Selected bond distances (nm) and bond angles (°) for compound 1

Fe(1)-O(1)	0.205 0(3)	Fe(1)-O(1)A	0.205 0(3)	Fe(1)-O(5)B	0.217 9(3)
Fe(1)-O(5)C	0.217 9(3)	Fe(1)-O(7)	0.229 2(4)	Fe(1)-O(7)A	0.229 2(4)
Fe(2)-O(2)	0.210 9(3)	Fe(2)-O(2)D	0.210 9(3)	Fe(2)-O(5)C	0.213 6(2)
Fe(2)-O(5)E	0.213 6(2)	Fe(2)-N(1)C	0.220 3(3)	Fe(2)-N(1)E	0.220 3(3)
O(1)-Fe(1)-O(1)A	141.53(17)	O(1)-Fe(1)-O(5)B	112.97(11)	O(1)-Fe(1)-O(5)C	91.45(10)
O(5)B-Fe(1)-O(5)C	101.82(14)	O(1)-Fe(1)-O(7)A	74.73(12)	O(1)A-Fe(1)-O(7)A	82.57(14)
O(5)B-Fe(1)-O(7)A	77.77(12)	O(5)C-Fe(1)-O(7)A	164.44(13)	O(1)-Fe(1)-O(7)	82.57(14)
O(1)A-Fe(1)-O(7)	74.73(12)	O(5)C-Fe(1)-O(7)	77.77(12)	O(7)A-Fe(1)-O(7)	106.8(2)
O(2)-Fe(2)-O(2)D	84.78(16)	O(2)-Fe(2)-O(5)C	87.23(10)	O(2)D-Fe(2)-O(5)C	94.22(10)
O(5)C-Fe(2)-O(5)E	178.03(14)	O(2)-Fe(2)-N(1)C	162.11(10)	O(2)D-Fe(2)-N(1)C	91.62(11)
O(5)C-Fe(2)-N(1)C	75.53(10)	O(5)E-Fe(2)-N(1)C	103.12(10)	N(1)C-Fe(2)-N(1)E	96.88(15)
Fe(2)F-O(5)-Fe(1)G	130.21(12)				

Symmetry transformations used to generate equivalent atoms: A: x, $-y+1/2$, $-z+1/2$; B: $x-1/2$, y, $-z$; C: $x-1/2$, $-y+1/2$, $z+1/2$; D: x, $-y+1/2$, $-z+3/2$; E: $x-1/2$, y, $-z+1$; F: $x+1/2$, y, $-z+1$; G: $x+1/2$, y, $-z$.

Table 3　Hydrogen bond lengths (nm) and angles (°) of complex 1

D–H···A	d(D-H)	d(H···A)	d(D···A)	∠DHA
O(3)–H(3)···O(6)A	0.082	0.186	0.268 3	176.0
O(7)–H(1W)···O(2)B	0.099	0.202	0.293 2	152.2

Symmetry code: A: $-x+3/2$, $-y+1$, $z+1$; B: x, $-y+1/2$, $-z+3/2$.

calculations were performed using the SHELXTL-97 system[17].

CCDC: 1437796.

2　Results and discussion

2.1　Crystal structure

The X-ray crystallography analysis reveals that the compound **1** crystallizes in the orthorhombic system space group *Pnna*. As shown in Fig.1, the asymmetric unit of **1** contains two crystallographically unique Fe(Ⅱ) atoms (half occupancy), one HL^{2-} ligand, and one coordinated H_2O molecule. Both Fe1 and Fe2 atoms possess a distorted octahedral coordination environment. The Fe1 center is coordinated by four O and two N atoms from the four different HL^{2-} blocks. The Fe2 center is also bound by four O atoms from the four different HL^{2-} ligands and two O atoms from two coordinated water molecules. The Fe-O (0.205 0(3) ~0.229 2(4) nm) and Fe-N (0.220 3(3) nm) bond lengths are in good agreement with those observed in

some other related Fe(Ⅱ) compounds[18-20]. In **1**, the HL^{2-} spacer exhibits a μ_4-coordination mode (Scheme 1), in which the two deprotonated carboxylate groups show the μ_2-η^1:η^1 and μ_2-η^2:η^0 bidentate modes. The dihedral angle between the pyridyl and phenyl rings in the HL^{2-} is 57.54°. The HL^{2-} moieties alternately link the adjacent Fe(Ⅱ) centers to form a 1D chain motif with the Fe⋯Fe separation of 0.391 4 (4) nm (Fig.2). These 1D motifs are arranged into a 2D sheet structure by further coordination interactions of the HL^{2-} ligands to Fe(Ⅱ) ions (Fig.2). For topological analysis[21-22], the 2D metal-organic network in **1** was simplified (terminal H_2O ligands omitted, μ_4-HL^{2-} moieties reduced to centroids) to give an underlying binodal 4,4-connected layer (Fig.3). It is built from the 4-connected topologically equivalent Fe1/Fe2 and μ_4-HL^{2-} nodes and features an topology[21-22] defined by the point symbol of $(4^3.6^2.8)$. Furthermore, the neighboring metal-organic sheets in **1** are assembled, through the O–H⋯O hydrogen bonds, into a 3D supramolecular framework (Fig.4)

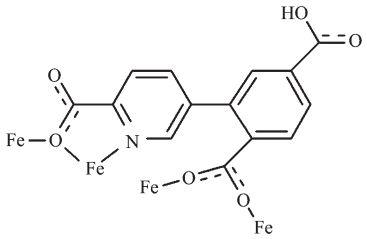

Scheme 1 Coordination mode of HL^{2-} ligand in compound **1**

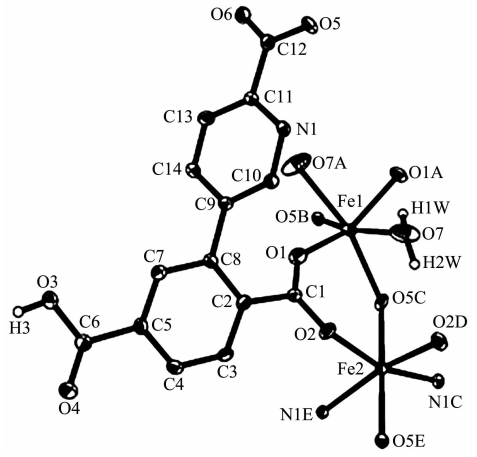

Symmetry codes: A: x, $-y+1/2$, $-z+1/2$; B: $x-1/2$, y, $-z$; C: $x-1/2$, $-y+1/2$, $z+1/2$; D: x, $-y+1/2$, $-z+3/2$; E: $x-1/2$, y, $-z+1$

Fig.1 Drawing of the asymmetric unit of compound **1**

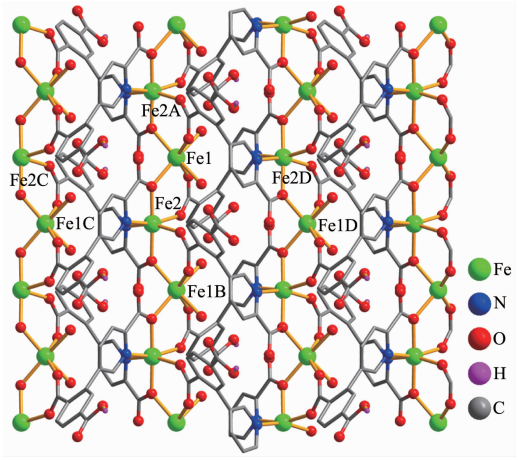

Symmetry code: A: x, y, $z-1$; B: x, y, $z+1$; C: $x-1/2$, y, $-z+1$; D: $x+1/2$, y, $-z+1$

Fig.2 Perspective of the 2D metal-organic sheet parallel to the *ac* plane

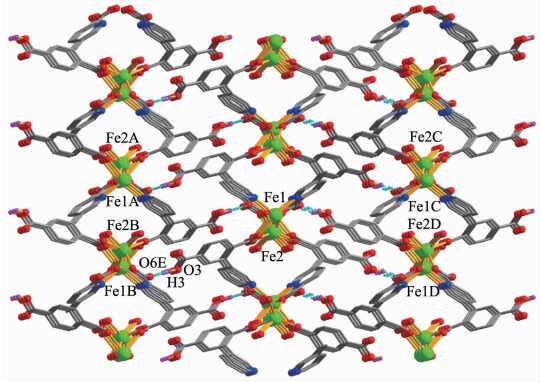

Dashed lines represent the H-bonds; Symmetry code: A: $-x+1/2$, $-y$, $z+1$; B: $-x+1$, $-y$, $-z+1$; C: $-x+1/2$, $-y+1$, $z+1$; D: $-x+1$, $-y+1$, $-z+2$; E: $-x+3/2$, $-y+1$, $z+1$

Fig.3 Perspective of the 3D supramolecular framework parallel to the *ab* plane

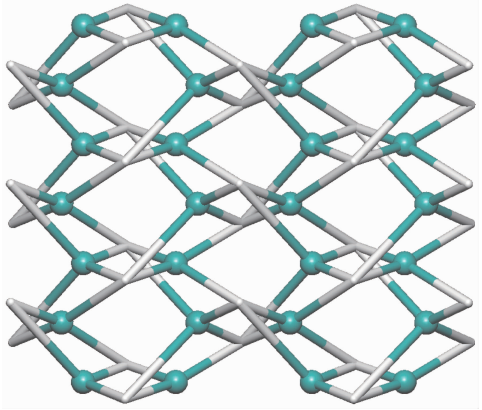

Fig.4 Topological representation of the underlying 2D metal-organic network showing a binodal 4,4-connected layer with the unique topology defined by the point symbol of $(4^3.6^2.8)$

2.2 TGA analysis and PXRD result

The thermal stability of compound **1** was investigated under nitrogen atmosphere by thermogravimetric analysis (TGA). As shown in Fig.5, the TGA curve of the compound **1** indicates that there is one distinct thermal effect in the 122~270 ℃ range, which corresponds to the removal of one coordinated H_2O molecule (Obsd. 5.1%; Calcd. 5.0%). Further heating up to 416 ℃ leads to the decomposition of dehydrated sample.

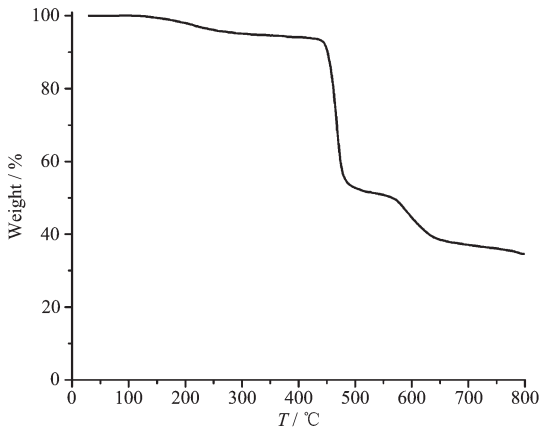

Fig.5 TGA curve of compound **1**

Powder X-ray diffraction (PXRD) experiment for compound **1** has been carried out at room temperature to identify whether the crystal structure can represent the bulk samples. As shown in Fig.6, the peak positions of the PXRD pattern closely match the simulated ones, thus indicating that the as-synthesized bulk material is pure product.

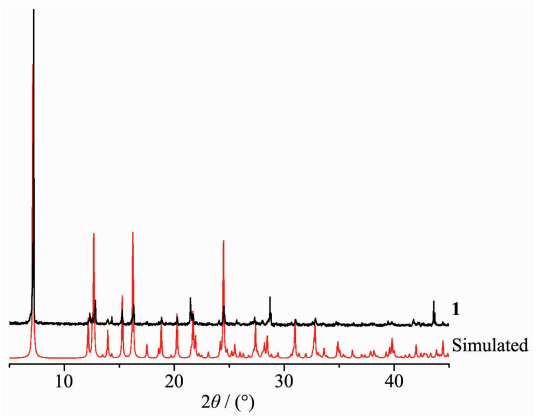

Fig.6 PXRD pattern of compound **1** at room temperature

2.3 Magnetic properties

Variable-temperature magnetic susceptibility studies were carried out on powder samples of **1** in the 2~300 K temperature range. As shown in Fig.7, the $\chi_M T$ value at 300 K is 3.61 cm^3·mol^{-1}·K, which is larger than the spin-only value 3.00 cm^3·mol^{-1}·K for a magnetically isolated high-spin Fe(Ⅱ) center (S=2, g=2.0), as expected for the presence of an orbital contribution in octahedral Fe(Ⅱ)[20,23]. As the temperature is lowered, the $\chi_M T$ values gradually decrease to 0.68 cm^3·mol^{-1}·K at 2.0 K, which indicates the presence of an antiferromagnetic interaction in **1**. Between 2.0 and 300 K, the magnetic susceptibility can be fitted to the Curie-Weiss law with C_M=3.64 cm^3·mol^{-1}·K and θ=−3.91 K. These results indicate an antiferromagnetic interaction between the adjacent Fe(Ⅱ) ions. According to the crystal structure of **1**, compound **1** can be considered as 1D chain from the viewpoint of magnetism due to long distance between the chain motifs. We tried to fit the magnetic data of **1** using the following expression for a 1D Fe(Ⅱ) chain[23-24]:

$$\chi_{chain}=\frac{N_A g^2 \mu_B^2 S(S+1)}{3kT}\frac{1+\mu}{1-\mu} \quad (1)$$

Where μ is the Langevin function:

$$\mu=\coth\frac{JS(S+1)}{kT}-\frac{kT}{S(S+1)} \quad (2)$$

And J is the parameter of exchange interaction between two Fe(Ⅱ) ions bridged by the carboxylate groups. Using this rough model, the susceptibilities for **1** were simulated, leading to J=−2.57 cm^{-1}, g=2.04, and the agreement factor R=5.19×10^{-5} ($R=\sum(\chi_{obs}T-\chi_{calc}T)^2/$

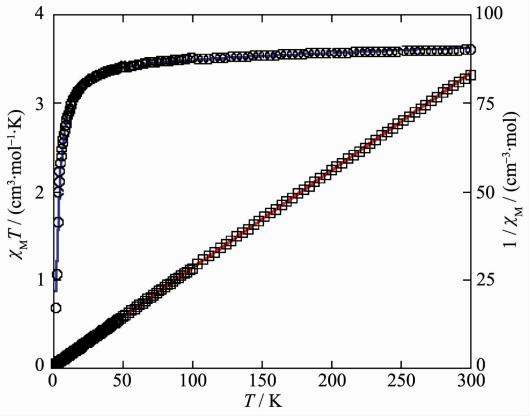

Curve represents the best fit to the equations in the text and the straight line shows the Curie-Weiss fitting

Fig.7 Temperature dependence of $\chi_M T$ (○) and $1/\chi_M$ (□) for compound **1**

$\sum(\chi_{obs}T)^2$). The negative J parameter confirms that an antiferromagnetic exchange coupling exists between the adjacent Fe(Ⅱ) centers, which is agreement with a negative θ value. There are two sets of magnetic exchange pathways within the chain motif, which consist of one carboxylate group in syn-syn fashion and one η^2-O bridge from the μ_2-carboxylate group, cooperatively contributed by the antiferromagnetic coupling transported by mixed bridges.

References:

[1] DeCoste J B, Peterson G W. *Chem. Rev.*, **2014**,**114**:5695-5727

[2] Kreno L E, Leong K, Farha O K, et al. *Chem. Rev.*, **2012**, **112**:1105-1125

[3] Zhang X W, Xing P Q, Geng X J, et al. *J. Solid State Chem.*, **2015**,**229**:49-61

[4] Liu L, Huang C, Xue X N, et al. *Cryst. Growth Des.*, **2015**, **15**:4507-4517

[5] Zhang Q F, Zhang H N, Zeng S Y, et al. *Chem. Asian J.*, **2013**,**8**:1985-1989

[6] Lu Z Z, Zhang R, Li Y Z, et al. *J. Am. Chem. Soc.*, **2010**, **133**:4172-4174

[7] Stock N, Biswas S. *Chem. Rev.*, **2012**,**112**:933-969

[8] Zhang L N, Zhang C, Zhang B, et al. *CrystEngComm*, **2015**, **17**:2837-2846

[9] Xu X X, Lu Y, Wang E B, et al. *Cryst. Growth Des.*, **2006**,**6**: 2029-2035

[10]Du M, Li C P, Liu C S, et al. *Coord. Chem. Rev.*, **2013**,**257**: 1282-1305

[11]Chen X M, Tong M L. *Acc. Chem. Res.*, **2007**,**40**:162-170

[12]Stepenson A M, Ward D. *Chem. Commun.*, **2012**,**48**:3605-3607

[13]Mahmudov K T, Kopylovich M N, Maharramov A M, et al. *Coord. Chem. Soc.*, **2014**,**265**:1-37

[14]WANG Ji-Wu(王继武), SU Yong-Chao(苏永超), WANG Ji-Jiang(王记江). *Chinese J. Struct. Chem.*(结构化学), **2015**, **34**(9):1385-1390

[15]DENG Ji-Hua(邓记华), ZHONG Di-Chang(钟地长), MEI Guang-Quan(梅光泉). *Chinese J. Inorg. Chem.*(无机化学学报), **2013**,**29**(1):175-179

[16]Gu J Z, Gao Z Q, Tang Y. *Cryst. Growth Des.*, **2012**,**12**: 3312-3323

[17]Sheldrick G M. *SHELXL NT Version* 5.1, *Program for Solution and Refinement of Crystal Structures*, University of Göttingen, Germany, **1997**.

[18]Lu W G, Gu J Z, Jiang L, et al. *Cryst. Growth Des.*, **2008**, **8**:192-199

[19]Han Y F, Song Y. *Inorg. Chem. Commun.*, **2015**,**55**:83-87

[20]Yao P F, Tao Y, Li H Y, et al. *Cryst. Growth Des.*, **2015**,**15**: 4394-4405

[21]Blatov V A. *IUCr CompComm Newsletter*, **2006**,**7**:4-38

[22]Blatov V A, Shevchenko A P, Proserpio D M. *Cryst. Growth Des.*, **2014**,**14**:3576-3586

[23]Su P, Lu L P, Feng S S, et al. *Dalton Trans.*, **2015**,**44**:7213-7222

[24]Fisher M E. *Am. J. Physiol.*, **1964**,**32**:343-346